Crystal Growth

DOI: 10.1002/anie.201000952

A Strategy for Retrospectively Mapping the Growth History of a Crystal**

Benjamin A. Palmer, Kenneth D. M. Harris, and François Guillaume**

Crystal growth processes[1] are ubiquitous in nature and play a crucial role in many chemical and industrial contexts. In order to be able to optimize and control crystal growth, it is essential to establish an understanding of the sequence of events involved in the growth process, rather than simply studying the morphological and structural properties of the bulk crystals collected at the end of the process. Knowledge of how crystals actually evolve during growth may be established directly by applying experimental techniques that allow crystal growth processes to be monitored in situ,[2] but for a variety of reasons, in situ studies may not be viable in many cases (e.g. due to limitations arising from the crystallization apparatus, the specific experimental conditions required, or the timescales involved). For these reasons, we were motivated to devize a strategy to allow insights to be gained on the evolution of crystal growth processes, based not on in situ measurements but based instead on the analysis of crystals recovered at the end of the process. Here we demonstrate a strategy that allows the growth history of a crystal to be established retrospectively, after the crystal has been collected at the end of the crystallization process.

Our strategy is based on a crystallization system for which the composition (C) of the growing surfaces of the crystal varies as a function of time $C(t)$ during the growth process, while the crystal structure remains constant with time. After collecting a crystal at the end of the growth process, the distribution of composition $C(X,Y,Z)$ within the crystal is measured and is interpreted to reveal details of the evolution of crystal growth. Thus, a three-dimensional contour at a specific value of composition $C(X,Y,Z) = C_i$ within the crystal defines the three-dimensional shape of the crystal at the specific time during the growth process at which the composition of the growing surfaces of the crystal was $C(t) = C_i$. Contours corresponding to different values of C_i thus provide a representation of the changes that occurred in the shape of the crystal as a function of time during growth. In some respects, the approach is analogous to establishing the growth characteristics of a tree retrospectively by observing the spatial variation of the rings of the tree (i.e. dendrochronology).

To demonstrate our strategy for retrospective mapping of crystal growth history, we consider solid inclusion compounds containing binary mixtures of guest molecules. Variation of composition in this case arises because the two types of guest compete for inclusion within the host structure during crystal growth, such that the relative proportions of the two types of guest incorporated into the crystal vary in a well-defined manner as a function of time. The host tunnel structure is independent of the relative proportions of the two types of guest, and the material grows as a single crystal even though the guest composition changes with time. We focus on urea inclusion compounds,[2d,3] in which guest molecules (typically based on *n*-alkane chains) are located within one-dimensional tunnels (Figure 1a) in a urea host structure.[4] The guest molecules are densely packed along the host tunnels (diameter[4c] ca. 5.5 Å), with a periodic repeat that is usually incommensurate[4b,5] with the repeat of the host structure (although some types of guest molecule[6] are found to form commensurate structures).

[*] B. A. Palmer, Prof. Dr. K. D. M. Harris
School of Chemistry, Cardiff University
Park Place, Cardiff CF10 3AT, Wales (UK)
Fax: (+44) 2920-870-416
E-mail: harriskdm@cardiff.ac.uk
Homepage: http://www.cardiff.ac.uk/chemy/contactsandpeople/academicstaff/harris.html
Dr. F. Guillaume
Groupe Spectroscopie Moleculaire, ISM
Université de Bordeaux, UMR 5255
351 cours de la Liberation, 33405 Talence Cedex (France)
E-mail: f.guillaume@ism.u-bordeaux1.fr
Homepage: http://spectro.ism.u-bordeaux1.fr/pages-web/fiche_gf.html

[**] We are grateful to J. L. Bruneel and D. Talaga (ISM, Bordeaux) for experimental assistance; Dr. C. E. Hughes for help in preparing Figure 1b; EPSRC for studentship support (to BAP); the Welsh Livery Guild for a Travel Grant (to BAP); the Conseil Régional d'Aquitaine and European Union (programme FEDER) for funding equipment of the Vibrational Spectroscopy and Imaging platform at ISM.

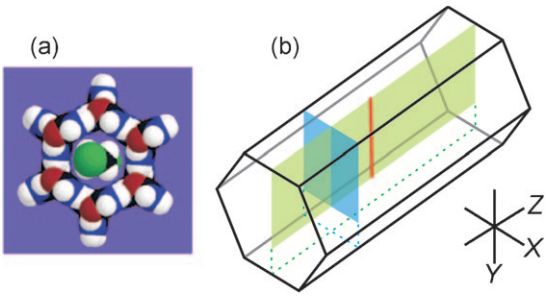

Figure 1. a) A single tunnel in a urea inclusion compound showing van der Waals radii and a 1,8-dibromooctane guest molecule. b) Schematic of a single crystal of a urea inclusion compound (needle morphology with hexagonal cross-section). The axis system is defined. The *Z*-axis is parallel to the tunnel direction of the urea host structure and the {100} faces are parallel to this axis. The incident laser in the confocal Raman microspectrometry experiments was parallel to the *Y*-axis. The different types of mapping carried out are indicated (red line, Figure 2; blue plane, Figure 3a; green plane, Figure 3b).

First we consider, in general terms, crystallization of a urea inclusion compound from a solution state containing two competing types of guest denoted A and B. The molar ratio of the two types of guest in solution at time t is $\gamma_A(t) = n_A(t)/n_B(t)$, where $n_i(t)$ is the number of moles of species i at time t. As discussed previously,[7] the molar ratio of guest molecules incorporated at the growing surfaces of the crystal at time t is

$$m_A(t) = \chi\,\gamma_A(t) \quad (1)$$

where χ depends on the relative affinity[8] of the host tunnel for inclusion of guests of types A and B. If inclusion of guests of type A is energetically favored over inclusion of guests of type B, then $\chi > 1$ and hence $m_A(t) > \gamma_A(t)$. Thus, the composition of the guest mixture incorporated within the growing surfaces of the crystal at time t [i.e. $m_A(t)$] has a higher proportion of guests of type A than the guest composition in the solution state at time t [i.e. $\gamma_A(t)$]. As a consequence, depletion of molecules of type A from the solution state occurs more rapidly than depletion of molecules of type B, and thus $\gamma_A(t)$ must decrease monotonically with time during crystal growth.[9] From Equation (1), $m_A(t)$ must also decrease monotonically with time, and thus the guest composition included at the growing crystal surfaces changes monotonically as a function of time.

After collecting a crystal at the end of the crystallization experiment, the spatial distribution $m_A(X,Y,Z)$ of the two types of guest in the crystal is measured. Contours at a specific value of m_A within the crystal can be related to a specific value of time during the crystal growth process (i.e. the time at which the composition of the growing crystal surfaces had the same specific value of m_A). As discussed above, $m_A(t)$ decreases monotonically with time, and thus lower values of $m_A(X,Y,Z)$ correspond to later stages of the crystal growth process, thus providing a basis for mapping the evolution of the growth of the crystal.

In the experiments discussed below, we focus on crystals of urea inclusion compounds containing mixtures of 1,8-dibromooctane (1,8-DBrO) and pentadecane (PD) guest molecules, with crystallization carried out using standard procedures (see Experimental Section). Confocal Raman microspectrometry was employed to measure the guest composition as a function of position within the crystal[10] [that is, $mA(X,Y,Z)$]. All results shown here were obtained from analysis of the same crystal (experiments on other crystals prepared under the same conditions confirm that the results are representative). PD and 1,8-DBrO were chosen as the guest mixture because they have different Raman signatures (see below) and because inclusion of PD within the urea tunnel structure is known to be energetically more favorable than inclusion of 1,8-DBrO. Previous studies of urea inclusion compounds by confocal Raman microspectrometry[12] (carried out in a different context[13] from the present work) have shown that spatial distributions of alkane and α,ω-dibromoalkane guests can be quantified by this technique. For quantitative analysis, we focus on the C–Br stretching ν(CBr) band for 1,8-DBrO (650 cm^{-1}; for the *trans* end-group conformation), the methyl rocking r(CH_3) band for PD (890 cm^{-1}) and the symmetric C–N stretching ν_s(CN) band for urea (1024 cm^{-1}). Guest composition is assessed from the ratio $R = I(\mathrm{CBr})/I(\mathrm{CN})$ of the integrated intensities of the ν(CBr) and ν_s(CN) bands, which is then normalized as $R_N = R/R_o$, where R_o is the value of R for the urea inclusion compound containing only 1,8-DBrO guests. The value of R_N establishes the relative amounts of 1,8-DBrO and PD guests in the probed region of the crystal, with higher R_N indicating a higher proportion of 1,8-DBrO. By definition, $0 \le R_N \le 1$, with the limiting values attained if only 1,8-DBrO ($R_N = 1$) or if only PD ($R_N = 0$) is present. The ratio $R_M = I(\mathrm{CH_3})/I(\mathrm{CN})$ of integrated intensities of the r(CH_3) and ν_s(CN) bands is also considered. Clearly, higher R_M corresponds to a higher proportion of PD guests in the probed region of the crystal.

The characteristic crystal morphology of conventional urea inclusion compounds is long needles with hexagonal cross-section (Figure 1b). The host tunnels are parallel to the needle axis (Z-axis). Confocal Raman microspectrometry involved one-dimensional or two-dimensional scans within the crystal as depicted (together with definition of the axis system) in Figure 1b. The incident laser was parallel to the Y-axis, and $Y = 0$ represents the upper surface of the crystal. Test experiments indicated that, for scans as a function of depth below the upper surface of the crystal (i.e. parallel to Y), reliable quantitative information is obtained only to a maximum depth of ca. 200 μm. For the crystal used to record the data shown here, the thickness of the crystal along the Y-axis was 250 μm. Thus, scans to a depth of 200 μm do not cover the full depth of the crystal, but do extend significantly below the center of the crystal. The length of the crystal along the Z-axis was 2170 μm.

Figure 2 shows results from a one-dimensional scan along the Y-axis (for fixed X and Z). The intensities of the ν(CBr) and r(CH_3) Raman bands (Figure 2a) change systematically as a function of depth (Y). Thus, ν(CBr) becomes stronger and r(CH_3) becomes weaker on moving from the interior of the crystal to the surface, while the intensities of the bands due to urea are essentially constant. Changes in the intensities of the ν(CBr) and r(CH_3) bands as a function of depth are quantified by R_N and R_M, respectively (Figure 2b). Because inclusion of PD is favored energetically over inclusion of 1,8-DBrO, the regions of the crystal formed at the earliest stages of growth have the highest proportion of PD (i.e. lowest R_N and highest R_M). Thus, the observed variations of R_N and R_M as a function of depth in the one-dimensional scan along the Y-axis (Figure 2b) are entirely consistent with the expectation that the region around the center of the crystal was formed at the earliest stage (i.e. lowest R_N) and the regions near the surface ($Y = 0$) were formed at the latest stage (i.e. highest R_N) of the crystal growth process.

More detailed insights on the evolution of the crystal growth process are obtained from two-dimensional scans (Figure 3). The XY-scan (in a plane perpendicular to the tunnel direction) in Figure 3a suggests that, at the specific value of Z probed in this scan, the earliest stage of the growth process (i.e. the region of lowest R_N) occurred close to the center of the final crystal ($X \approx 0$ μm, $Y \approx 150$ μm). The outer regions of the crystal (with $R_N > 0.5$ in Figure 3a) show clear evidence for the development of the hexagonal cross-section

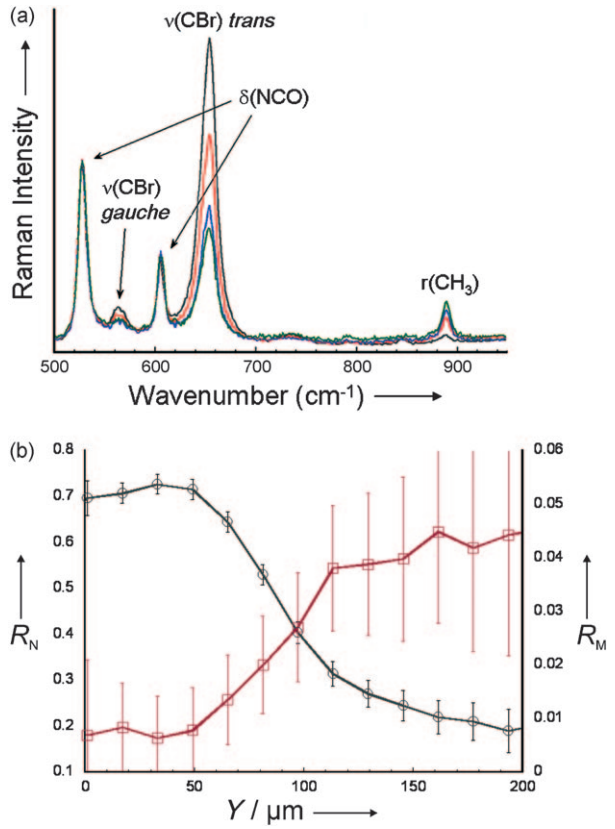

Figure 2. a) Raman spectra recorded at different depths (black, $Y=47$ μm; red, $Y=87$ μm; blue, $Y=129$ μm; green, $Y=170$ μm) below the upper surface of the crystal, showing systematic changes in the intensities of the ν(CBr) and r(CH_3) bands. b) Values of R_N and R_M determined as a function of depth (Y).

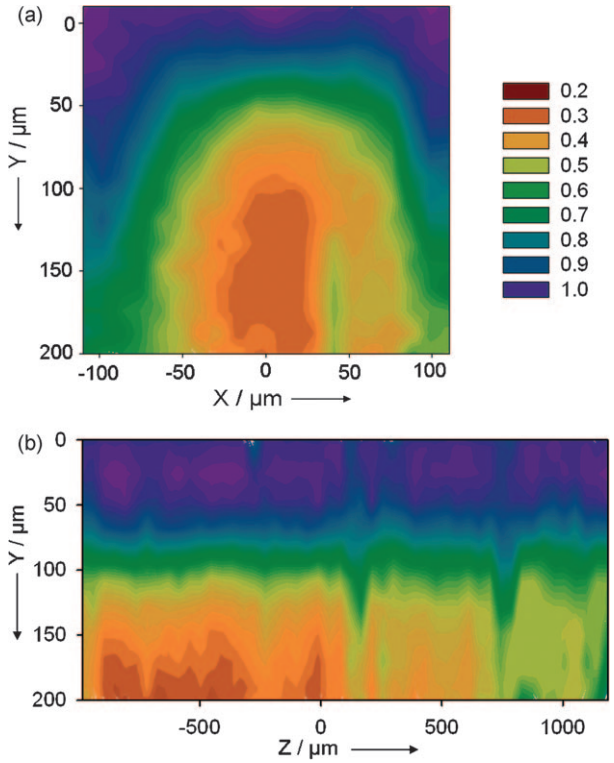

Figure 3. Results from a) an *XY*-scan (with Z fixed at $Z=0$ μm), and b) a *ZY*-scan (with X fixed at $X=0$ μm), showing the value of R_N determined from the Raman spectra recorded as a function of position within the crystal. In (b), the tunnel direction is horizontal (Z-axis). The color scheme for values of R_N is defined in the inset.

of the crystal shape (the characteristic growth morphology of urea inclusion compounds), with essentially equal rates of growth of the symmetry-related {100} faces. Clearly, the spacing between contours in maps of this type may be interpreted (at least qualitatively) in terms of the relative rates of growth of the crystal in different directions.

In the *ZY*-scan (Figure 3b), the region corresponding to the earliest stages of crystal growth (with $R_N \approx 0.2$) is identified as the bottom left part of the map. Significantly, this region is close to one end of the crystal along the Z-axis (horizontal), suggesting that the embryonic stages of growth were initiated close to one end of the final crystal and that subsequent growth along the tunnel occurred predominantly in one direction (from left to right in Figure 3b). In principle, the relative rates of crystal growth perpendicular (Y-axis) and parallel (Z-axis) to the tunnel may vary as the composition of the crystal changes. Thus, during the early stages of crystal growth corresponding to $R_N \leq 0.6$, the spacing between R_N contours is substantially greater along the Z-axis (to the right hand side of the region with $R_N \approx 0.2$ in Figure 3b) than along the Y-axis, indicating faster crystal growth along the tunnel direction (Z). In fact, at the stage of the growth process corresponding to $R_N \approx 0.6$, the crystal had already reached close to its final length along the tunnel direction but was still comparatively thin along Y. In the later stages of growth corresponding to $R_N > 0.6$, the contours are nearly parallel to the Z-axis, suggesting that, in this stage of the process, the growth of the crystal occurred predominantly perpendicular to the tunnel direction, leading to an increase in the width of the crystal (along Y) with no significant change in the length of the crystal along the tunnel direction.

The results reported here demonstrate the feasibility of the proposed strategy for retrospective mapping of the evolution of crystal growth processes. Although the interpretations are restricted to a qualitative level in the present case, our results have nevertheless revealed new insights regarding the crystal growth of urea inclusion compounds, particularly from the analysis of the *ZY*-scan discussed above. Our ongoing research to further advance this strategy, including the development of models to correlate the time-dependences of $m_A(t)$ and $\gamma_A(t)$, will allow substantially greater quantitative insights to be established. Although the strategy has been demonstrated for crystal growth of urea inclusion compounds, it may also be applied to a much wider range of materials, including solid solutions that are isostructural across the complete range of composition and a wide variety of different types of solid inclusion compound (such as gas hydrates, zeolites and other microporous inorganic solids, and metal–organic framework materials). In all of these cases, the strategy reported here for retrospective mapping of crystal growth has the potential to yield valuable insights on mechanistic aspects of the crystal growth process, and for

allowing different growth mechanisms to be distinguished, particularly when the results are considered in conjunction with those from in situ, time-resolved studies of the same crystal growth process.

Experimental Section

Crystallization of urea inclusion compounds containing PD and 1,8-DBrO guests was carried out by dissolving urea, PD, and 1,8-DBrO in methanol at 55 °C and cooling the solution to 20 °C over ca. 29 h. We focus on the specific case[14] with an initial 1,8-DBrO:PD molar ratio in the solution state of 95:5. Confocal Raman microspectrometry was carried out on a single crystal using a Labram II spectrometer (Jobin–Yvon) with an Ar/Kr 2018 Spectra–Physics laser (514.5 nm) and a grating of 1800 lines mm^{-1} (spectral resolution ca. 6 cm^{-1}). The laser was focused on the crystal through a microscope (50× Olympus objective; 0.55 numerical aperture; confocal pinhole diameter, 500 μm). Radial and axial resolutions (at a depth of ca. 100 μm) were both 10 μm. The *XY*-scan (Figure 3a) was measured in steps of 24.5 μm along *X* and 13.8 μm along *Y*. The *ZY*-scan (Figure 3b) was measured in steps of 44.3 μm along *Z* and 13.8 μm along *Y*. Values of *Y* (i.e. the depth of the focusing point below the upper surface of the crystal) were corrected to take account of the refractive index ($n \approx 1.5$)[15] of the material.

Received: February 15, 2010
Published online: June 16, 2010

Keywords: crystal growth · growth history · Raman microspectrometry · solid solutions · urea inclusion compounds

[1] a) "Crystal Growth and Nucleation": *Faraday Discuss.* **2007**, *136*; b) B. Kahr, J. M. McBride, *Angew. Chem.* **1992**, *104*, 1–28; *Angew. Chem. Int. Ed. Engl.* **1992**, *31*, 1–26; c) S. Mann, *Science* **1993**, *261*, 1286–1292; d) S. D. Durbin, G. Feher, *Annu. Rev. Phys. Chem.* **1996**, *47*, 171–204; e) S. Mann, *Angew. Chem.* **2000**, *112*, 3532–3548; *Angew. Chem. Int. Ed.* **2000**, *39*, 3392–3406; f) I. Weissbuch, M. Lahav, L. Leiserowitz, *Cryst. Growth Des.* **2003**, *3*, 125–150; g) N. E. Chayen, *Curr. Opin. Struct. Biol.* **2004**, *14*, 577–583; h) J. A. Dirksen, T. A. Ring, *Chem. Eng. Sci.* **1991**, *46*, 2389–2427; i) *Crystallization Process Systems* (Ed.: A. G. Jones), Elsevier, Amsterdam, **2002**; j) D. Erdemir, A. Y. Lee, A. S. Myerson, *Curr. Opin. Drug Discov. Devel.* **2007**, *10*, 746–755; k) S. Mann, *Angew. Chem.* **2008**, *120*, 5386–5401; *Angew. Chem. Int. Ed.* **2008**, *47*, 5306–5320; l) T. H. Zhang, X. Y. Liu, *Angew. Chem.* **2009**, *121*, 1334–1338; *Angew. Chem. Int. Ed.* **2009**, *48*, 1308–1312; m) M. R. Walsh, C. A. Koh, E. D. Sloan, A. K. Sum, D. T. Wu, *Science* **2009**, *326*, 1095–1098.

[2] a) F. Rey, G. Sankar, J. M. Thomas, P. A. Barrett, D. W. Lewis, C. R. A. Catlow, S. M. Clark, G. N. Greaves, *Chem. Mater.* **1995**, *7*, 1435–1436; b) G. Sankar, J. M. Thomas, F. Rey, G. N. Greaves, *J. Chem. Soc. Chem. Commun.* **1995**, 2549–2550; c) C. A. Koh, J. L. Savidge, C. C. Tang, *J. Phys. Chem.* **1996**, *100*, 6412–6414; d) M. D. Hollingsworth, M. E. Brown, A. C. Hillier, B. D. Santarsiero, J. D. Chaney, *Science* **1996**, *273*, 1355–1359; e) M. D. Ward, *Chem. Rev.* **2001**, *101*, 1697–1726; f) H. Groen, K. J. Roberts, *J. Phys. Chem. B* **2001**, *105*, 10723–10730; g) H. G. Alison, R. J. Davey, J. Garside, M. J. Quayle, G. J. T. Tiddy, D. T. Clarke, G. R. Jones, *Phys. Chem. Chem. Phys.* **2003**, *5*, 4998–5000; h) T. Uchida, S. Takeya, L. D. Wilson, C. A. Tulk, J. A. Ripmeester, J. Nagao, T. Ebinuma, H. Narita, *Can. J. Phys.* **2003**, *81*, 351–357; i) C. E. Hughes, K. D. H. Harris, *J. Phys. Chem. A* **2008**, *112*, 6808–6810; j) M. Shoaee, M. W. Anderson, M. R. Attfield, *Angew. Chem.* **2008**, *120*, 8653–8656; *Angew. Chem. Int. Ed.* **2008**, *47*, 8525–8528; k) M. Bremholm, M. Felicissimo, B. B. Iversen, *Angew. Chem.* **2009**, *121*, 4882–4885; *Angew. Chem. Int. Ed.* **2009**, *48*, 4788–4791.

[3] a) L. C. Fetterly in *Non-Stoichiometric Compounds*, Academic Press, New York, **1964**, pp. 491–567; b) K. Takemoto, N. Sonoda in *Inclusion Compounds*, Vol. 2, Academic Press, New York, **1984**, pp. 47–67; c) K. D. M. Harris, *J. Solid State Chem.* **1993**, *106*, 83–98; d) K. D. M. Harris, *J. Mol. Struct.* **1996**, *374*, 241–250; e) K. D. M. Harris, *Chem. Soc. Rev.* **1997**, *26*, 279–289; f) F. Guillaume, *J. Chim. Phys. (Paris)* **1999**, *96*, 1295–1315; g) M. D. Hollingsworth, *Science* **2002**, *295*, 2410–2413; h) K. D. M. Harris, *Supramol. Chem.* **2007**, *19*, 47–53.

[4] a) A. E. Smith, *Acta Crystallogr.* **1952**, *5*, 224–235; b) K. D. M. Harris, J. M. Thomas, *J. Chem. Soc. Faraday Trans.* **1990**, *86*, 2985–2996; c) A. R. George, K. D. M. Harris, *J. Mol. Graphics* **1995**, *13*, 138–141.

[5] a) A. J. O. Rennie, K. D. M. Harris, *Proc. R. Soc. London Ser. A* **1990**, *430*, 615–640; b) D. Schmicker, S. van Smaalen, J. L. de Boer, C. Haas, K. D. M. Harris, *Phys. Rev. Lett.* **1995**, *74*, 734–737; c) S. van Smaalen, K. D. M. Harris, *Proc. R. Soc. London Ser. A* **1996**, *452*, 677–700; d) R. Lefort, J. Etrillard, B. Toudic, F. Guillaume, T. Breczewski, P. Bourges, *Phys. Rev. Lett.* **1996**, *77*, 4027–4030; e) J. Ollivier, C. Ecolivet, S. Beaufils, F. Guillaume, T. Breczewski, *Europhys. Lett.* **1998**, *43*, 546–551; f) R. Lefort, B. Toudic, J. Etrillard, F. Guillaume, P. Bourges, R. Currat, T. Breczewski, *Eur. Phys. J. B* **2001**, *24*, 51–57.

[6] a) M. D. Hollingsworth, B. D. Santarsiero, K. D. M. Harris, *Angew. Chem.* **1994**, *106*, 698–701; *Angew. Chem. Int. Ed. Engl.* **1994**, *33*, 649–652; b) M. E. Brown, J. D. Chaney, B. D. Santarsiero, M. D. Hollingsworth, *Chem. Mater.* **1996**, *8*, 1588–1591; c) M. D. Hollingsworth, U. Werner-Zwanziger, M. E. Brown, J. D. Chaney, J. C. Huffman, K. D. M. Harris, S. P. Smart, *J. Am. Chem. Soc.* **1999**, *121*, 9732–9733; d) M. D. Hollingsworth, M. E. Brown, M. Dudley, H. Chung, M. L. Peterson, A. C. Hillier, *Angew. Chem.* **2002**, *114*, 1007–1011; *Angew. Chem. Int. Ed.* **2002**, *41*, 965–969; e) S.-O. Lee, B. M. Kariuki, K. D. M. Harris, *Angew. Chem.* **2002**, *114*, 2285–2288; *Angew. Chem. Int. Ed.* **2002**, *41*, 2181–2184; f) S.-O. Lee, B. M. Kariuki, K. D. M. Harris, *New J. Chem.* **2005**, *29*, 1266–1271.

[7] a) K. D. M. Harris, P. E. Jupp, *Proc. R. Soc. London Ser. A* **1997**, *453*, 333–352; b) K. D. M. Harris, P. E. Jupp, S.-O. Lee, *J. Chem. Phys.* **1999**, *111*, 9784–9791; c) S.-O. Lee, K. D. M. Harris, P. E. Jupp, L. Yeo, *J. Am. Chem. Soc.* **2001**, *123*, 12913–12914; d) A. M. Pivovar, K. T. Holman, M. D. Ward, *Chem. Mater.* **2001**, *13*, 3018–3031.

[8] We note that $m_A(t)$ is the instantaneous value of the guest molar ratio. The overall guest ratio within the crystal at time *t* is given by integration of $m_A(t)$ from the start of the growth of the crystal ($t = 0$) until time *t*.

[9] Clearly, $\gamma_A(t)$ decreases until all guest molecules of type A initially present in the solution state have been included within the crystal. At this stage, and during any subsequent crystal growth, $\gamma_A(t) = 0$ and hence $m_A(t) = 0$.

[10] Although crystallization of urea inclusion compounds containing binary mixtures of different types of guest molecule has been carried out previously for a variety of different purposes,[6b,c,11] to our knowledge the present work represents the first time that the spatial distribution of the two types of guest in such materials has actually been explored.

[11] a) M. D. Hollingsworth, N. Cyr, *Mol. Cryst. Liq. Cryst.* **1990**, *187*, 135–144; b) Q. Y. Shang, X. M. Dou, B. S. Hudson, *Nature* **1991**, *352*, 703–705; c) M. E. Brown, M. D. Hollingsworth, *Nature* **1995**, *376*, 323–327; d) T. Weber, H. Boysen, F. Frey, *Acta Crystallogr. Sect. B* **2000**, *56*, 132–141; e) D. G. Hayes, J. VanAlstine, A. L. Asplund, *Sep. Sci. Technol.* **2001**, *36*, 45–58.

[12] a) J. Marti-Rujas, A. Desmedt, K. D. M. Harris, F. Guillaume, *J. Am. Chem. Soc.* **2004**, *126*, 11124 – 11125; b) J. Martí-Rujas, K. D. M. Harris, A. Desmedt, F. Guillaume, *J. Phys. Chem. B* **2006**, *110*, 10708 – 10713; c) J. Martí-Rujas, A. Desmedt, K. D. M. Harris, F. Guillaume, *J. Phys. Chem. B* **2007**, *111*, 12339 – 12344; d) J. Martí-Rujas, A. Desmedt, K. D. M. Harris, F. Guillaume, *J. Phys. Chem. C* **2009**, *113*, 736 – 743.

[13] Previous work was focused on mechanistic and kinetic aspects of guest exchange processes, and did not investigate materials containing binary mixtures of guest molecules prepared by crystallization processes.

[14] Inclusion of PD is significantly more favorable than inclusion of 1,8-DBrO, and thus $\chi >> 1$. Under these conditions, it is necessary to start the crystallization experiment with a low relative proportion of PD guests in the solution state [i.e. a low value of $\gamma_A(0)$, where A represents PD] in order for a significant range of *mA* values to be observed within the crystal during the growth process.

[15] D. Schmicker, S. van Smaalen, C. Haas, K. D. M. Harris, *Phys. Rev. B* **1994**, *49*, 11572 – 11579.

